Effect of chain length on fragility and thermodynamic scaling of the local segmental dynamics in poly(methylmethacrylate)

R. Casalini
Chemistry Department, George Mason University, Fairfax, Virginia 22030 and Chemistry Division, Code 6120, Naval Research Laboratory, Washington, DC 20375-5342

C. M. Roland
Chemistry Division, Code 6120, Naval Research Laboratory, Washington, DC 20375-5342

S. Capaccioli
Dipartimento di Fisica, Università di Pisa, Pisa, Largo B. Pontecorve 3, I-56127, Italy and CNR-INFM, CRS SOFT, Università di Roma "La Sapienza," Piazzale Aldo Moro 2, 00185, Roma, Italy

(Received 29 January 2007; accepted 20 March 2007; published online 11 May 2007)

Local segmental relaxation properties of poly(methylmethacrylate) (PMMA) of varying molecular weight are measured by dielectric spectroscopy and analyzed in combination with the equation of state obtained from *PVT* measurements. Significant variations of glass transition temperature and fragility with molecular weight are observed. In accord with the general properties of glass-forming materials, single molecular weight dependent scaling exponent γ is sufficient to define the mean segmental relaxation time τ_α and its distribution. This exponent can be connected to the Grüneisen parameter and related thermodynamic quantities, thus demonstrating the interrelationship between dynamics and thermodynamics in PMMA. Changes in the relaxation properties ("dynamic crossover") are observed as a function of both temperature and pressure, with τ_α serving as the control parameter for the crossover. At longer τ_α another change in the dynamics is apparent, associated with a decoupling of the local segmental process from ionic conductivity. © *2007 American Institute of Physics*. [DOI: 10.1063/1.2728898]

INTRODUCTION

The chain connectivity of polymers introduces complexities that make their behavior distinct from that of molecular liquids. For example, the uncrossability of long chains gives rise to entanglement constraints, which confer shear thinning and marked viscoelasticity to the low frequency dynamics; these effects are generally absent in small molecules. On the other hand, the structural relaxation properties of polymers and molecular liquids, usually measured at higher frequencies, are virtually indistinguishable. The dynamics of both materials exhibit a dramatic slowing down upon approach to the glass transition, which is unaccompanied by any marked change in structure or molecular configuration. A common structural relaxation property is the fragility, $m = \partial \log(\tau_\alpha)/\partial(T_g/T)|_{T=T_g}$, quantifying the temperature dependence of the structural relaxation time τ_α.[1] Polymers tend to be somewhat more fragile (larger m) than molecular liquids, although there are exceptions.[2] The fragility of polymers can vary with their molecular weight (M_w). For example, m increases with M_w for polystyrene (PS),[3–5] poly(methymethacrylate) (PMMA),[6] polypropylene glycol (PPG),[7] and methyl-terminated PPG (which lacks H bonds).[8] More flexible chain polymers, such as polydimethylsiloxane[9] (PDMS) and polyphenylmethylsiloxane (PMPS),[10] lack this sensitivity of m to M_w. This is consistent with the observation that less flexible chains and those having bulky pendant groups tend to exhibit a more fragile behavior.[11] This effect is ascribed to stronger intermolecular constraints for the latter, as effected also by cross-linking.[12]

Although fragility quantifies the temperature dependence of the relaxation time, since an isobaric temperature variation also changes the density, m provides no information about whether the dynamics are thermally activated or governed more by the volume changes accompanying changes in T. In particular, for van der Waals polymers, shorter chains appear to allow easier segmental rearrangements, so that volume exerts a stronger effect for decreasing M_w.[13] A method used to quantify the relative influence of temperature T and specific volume V on the structural dynamics is the ratio of the isochoric activation energy to the isobaric activation enthalpy, $E_V/H_P = [\partial \log(\tau)/\partial(1/T)|_V]/[\partial \log(\tau)/\partial(1/T)|_P]$, by convention evaluated at the glass transition,[14–16] but also determinable as a function of T and P.[13,15,17,18] This ratio varies between 0 and 1 for the limiting cases of volume- and temperature-dominated dynamics, respectively. Compilations of E_V/H_P for many materials have been published.[19–22] For hydrogen bonded materials E_V/H_P is close to unity, while for van der Waals molecules this ratio is smaller ($0.38 \leqslant E_V/H_P \leqslant 0.6$); polymers exhibit intermediate values ($0.25 \leqslant E_V/H_P \leqslant 0.86$).

Very flexible chains, such as those with oxygen in the backbone, have low ratios, for example, $E_V/H_P = 0.56$ and 0.52, respectively, for PDMS and PMPS. As temperature is increased above T_g, E_V/H_P decreases.[13,15,17,18] This leads to an exceptionally low value of $E_V/H_P = 0.25$ for poly(2,6-dimethyl-1,4-phenylene oxide),[23] which combines a flexible backbone and an unusually high glass transition temperature ($T_g = 461.8$ K).

An alternative approach to evaluating temperature and volume dependences is by thermodynamical scaling of relaxation times.[24] For each material there is a constant γ such that

$$\log(\tau_\alpha) = \mathfrak{J}(TV^\gamma). \tag{1}$$

This scaling behavior is observed very generally for nonassociated organic glass formers (the exceptions being materials with extensive hydrogen bonding).[25] Equation (1) can be derived from the consideration of the T and V dependences of the entropy.[26–28] It follows from the idea that the repulsive part of the intermolecular potential dominates the local liquid structure,[29,30] so that for local properties the potential can be approximated with a spherically symmetric, two-body interaction,[30–32]

$$U(r) = \varepsilon\left(\frac{\sigma}{r}\right)^{3\gamma} - \frac{a}{r^3}, \tag{2}$$

where ε and σ are the characteristic energy and length scale of the system and r is the intermolecular distance. The mean-field parameter a describes the long-range attractive potential, which can be taken as a constant when considering local properties, such as the structural relaxation in liquids or the local segmental relaxation of polymers. Recent simulations of the glass transition have employed this inverse power repulsive potential.[29,30,33] Molecular dynamic simulations of 1,4-polybutadiene, employing a potential given by the superposition of a 6-12 Lennard-Jones intermolecular potential and harmonic chain stretching and bending potentials, yield the scaling behavior [Eq. (1)] with $\gamma=2.8$.[34,35]

These results imply that for low molecular weight polymers, the potential is much closer to that of a monomer, approaching the spherically symmetric form of Eq. (2), while for higher molecular weight the contribution of the intramolecular forces, modeled with additional harmonic terms,[25] is more significant. The effect of the latter is to reduce the steepness of the effective potential, with consequently lower γ for high molecular weight polymers.

There is a simple relation between the scaling exponent γ and the activation enthalpy ratio[24,36]

$$\left.\frac{E_V}{H_P}\right|_{T_g} = (1 + \gamma\alpha_P T_g)^{-1}, \tag{3}$$

where $\alpha_P(=\partial \ln(V)/\partial T|_P)$ is the isobaric thermal expansion coefficient. Since the product $\alpha_P T_g$ is approximately constant for different materials [$=0.18\pm0.02$ (Refs. 37 and 38)], γ has an inverse relationship to E_V/H_P. Since γ is constant and $\alpha_P T$ generally increases with T, the reduction in E_V/H_P with T, referred to above, follows directly from Eq. (3);[13] that is, volume becomes more important as temperature increases further above T_g. Since the ratio E_V/H_P can be calculated directly from the pressure and temperature dependences of the volume,[39] using Eq. (3) γ can be obtained without making relaxation measurements (i.e., from just thermodynamic data).[13]

In this work we measured structural relaxation times as a function of temperature and pressure, along with the equation of state, for three oligomers of PMMA. From these data we investigate the effect of chain length on the thermodynamical scaling and thus on the structural relaxation properties E_V/H_P, γ, and fragility.

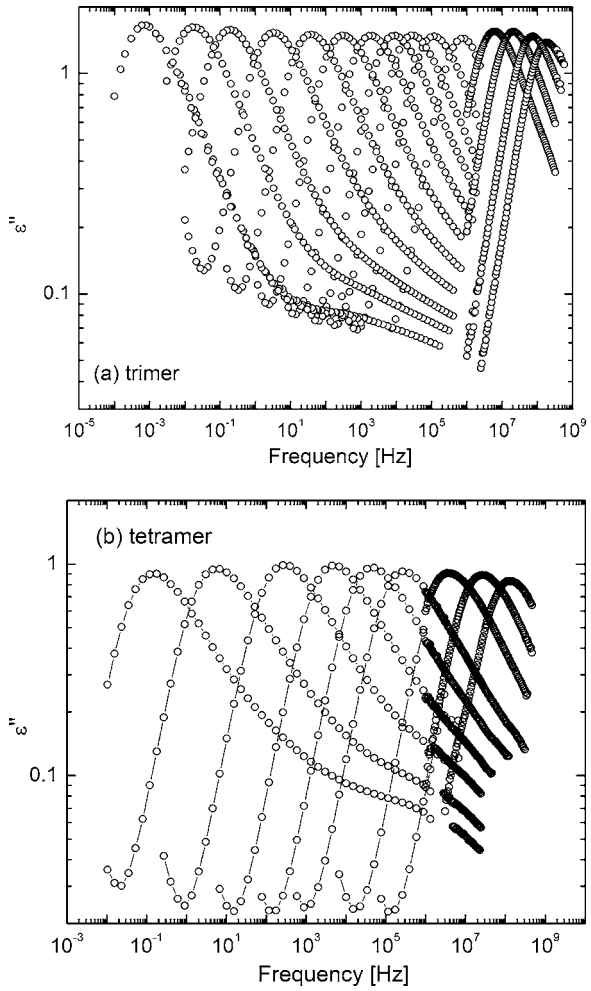

FIG. 1. (a) Selected dielectric loss spectra for the trimer measured at atmospheric pressure for temperatures (from left to right): 211, 215, 218, 223, 228, 233, 238, 243, 248, 253, and 262 K. (b) Selected dielectric loss spectra for the tetramer measured at atmospheric pressure for temperatures (from left to right): 246, 253, 263, 273, 283, 293, 313, 333, and 358 K.

EXPERIMENT

The three hydrogen-terminated PMMA (from Polymer Standard Service) had degrees of polymerization (n) equal to 3, 4, and 10, with weight average molecular weights of M_w = 302 g/mol (trimer), M_w=402 g/mol (tetramer), and M_w = 1040 g/mol (decamer). The lower M_w samples were monodisperse, while the decamer had a polydispersity=1.3. All samples were used as received.

Pressure-volume-temperature (PVT) measurements were carried out with a Gnomix instrument.[40] At room temperature solid samples were molded under vacuum into a cylinder, while liquid samples were injected directly into the cell. The temperature was raised at 0.5 K/min at various fixed pressures up to 200 MPa. The ambient density was measured by the buoyancy method for the decamer and tetramer and volumetrically for the trimer.

For the tetramer, ambient pressure dielectric spectra (10^{-2}–10^6 Hz) were measured with a Novocontrol Alpha

analyzer using a parallel plate configuration. Temperature was controlled using the Novocontrol Quatro cryosystem (±0.01 K stability). Dielectric measurements on the other PMMA samples were carried out with the Alpha analyzer, as well as an IMASS time domain dielectric analyzer (10^{-4}–10^{3} Hz) and an HP16453A test fixture with an HP4291A impedance analyzer (10^{6}–10^{9} Hz). For these measurements at $f<10^{6}$ Hz, a closed-cycle helium cryostat with a helium atmosphere was used for temperature control to within ±0.02 K. Measurements above 10^{6} Hz employed an ESPEC SH-240 temperature chamber in a nitrogen atmosphere.

For dielectric measurements at elevated pressure, the sample was contained in a Harwood Engineering pressure vessel, with hydraulic pressure applied using an Enerpac pump in combination with a pressure intensifier (Harwood Engineering). Pressures were measured with a Sensotec tensometric transducer (resolution=150 kPa). The sample assembly was contained in a Tenney, Jr. temperature chamber, with control to within ±0.1 K at the sample.

Differential scanning calorimetry (DSC) employed a TA Instruments Q100 using liquid nitrogen cooling. Samples were cooled from the liquid state to below T_g at 10 K/min. The absolute value of the heat capacity was obtained using a synthetic sapphire for calibration.[41]

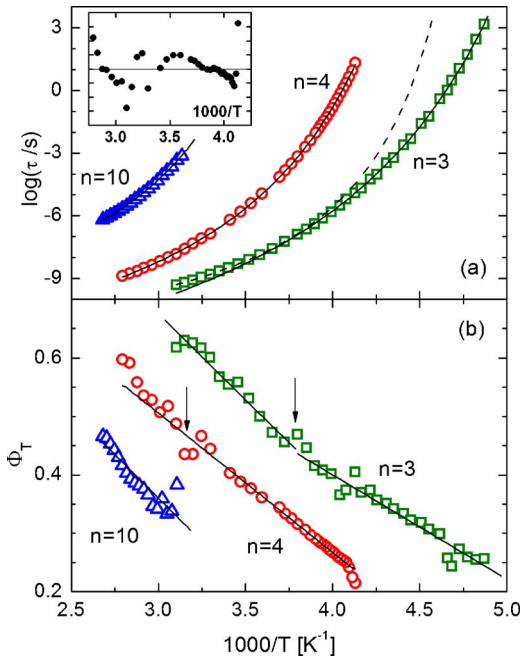

FIG. 2. (a) α-relaxation time for PMMA oligomers having the indicated number of repeat units. The solid lines represent the VFTH equation, with the parameters given in Table I. The inset shows the deviation between the VFTH and the experimental data for the tetramer. (b) Stickel derivative plots. The arrows indicate the dynamic crossover, corresponding to the intersection of the fitted lines for the trimer and the deviation from the VFTH for the tetramer.

RESULTS

Dynamic crossover

Figures 1(a) and 1(b) show representative dielectric loss spectra for the trimer and tetramer, respectively, measured at atmospheric pressure. Comparing to spectra in the literature for high molecular weight PMMA,[42,43] a clear difference is evident in the dielectric strength of the secondary relaxation relative to that of the α relaxation. For high molecular weight PMMA the intensity of the secondary relaxation is larger than that of the structural relaxation, while for the oligomers it is much smaller, whereby it can be clearly resolved only in the vicinity of the glass transition. The effect of molecular weight and pressure on the secondary relaxation of PMMA will be discussed in detail in a subsequent publication; the focus herein is the α relaxation.

The breadth of the α peaks in Fig. 1 decreases with temperature. A structural relaxation time (the most probable relaxation time τ_α) can be defined from the maximum of the loss peak, with the latter determined by fitting the peak to a Havriliak-Negami function.[44] Any contribution from the secondary relaxation for the trimer and tetramer was neglected. For the decamer the spectra were analyzed using a single function only at higher temperatures where the secondary and structural peaks cannot be distinguished.

In Fig. 2(a) are the temperature dependences of τ_α for the three oligomers, with the variation of T_g over this range of M_w evident A function to describe the temperature dependence of the relaxation time at constant pressure is the Vogel-Fulcher-Tamman-Hesse (VFTH) equation[45,46]

$$\tau(T) = \tau_0 \exp\left(\frac{DT_0}{T - T_0}\right), \tag{4}$$

where T_0, the Vogel temperature, D, and τ_0 are constants. The validity of this equation is usually limited to temperatures close to the glass transition since for shorter τ_α (in the range of 10^{-4}–10^{-7} s) a second VFTH is required.[47–51] This deviation from Eq. (4), referred to as the "dynamic crossover," is revealed using the derivative function

$$\phi_T = \{d[\log(\tau_\alpha)]/d[1000/T]\}^{-1/2} \tag{5}$$

introduced by Stickel *et al.*[49] ϕ_T is a single straight line for data conforming to Eq. (4). In Fig. 2(b) ϕ_T is displayed for the three oligomers. The trimer exhibits a change in dynamics at a temperature $T_B=264\pm5$ K corresponding to $\log(\tau_B)=-6.9\pm0.3$, as determined from the intersection of the two linear fits to the derivative data. For the tetramer a change in dynamics is less obvious, as seen in Fig. 2(a), its relaxation times can be described by a single VFTH over the entire range (see inset). The Stickel plot for the tetramer gives a hint of a crossover at $T_B\sim316$ K corresponding to $\log(\tau_B)\sim-7.5$, but the uncertainty is large. For the decamer the range of the data is more limited, and only a single VFTH is required to fit the τ_α. All parameters and values of T_B are listed in Table I.

Ionic conductivity

In the analysis of the loss spectra the dc-conductivity contribution from the presence of mobile ions in the polymer was included as an inverse power law, $\varepsilon_{dc}(\omega)=-i\sigma/\omega\varepsilon_0$,

TABLE I. Fit parameters for Eq. (4).

n	$\log(\tau_0/s)$	T_0 (K)	D	m[a]
3 ($T<T_B$=264 K)	−14.5±0.2	161.6±1	11.0±0.4	74±2
3 ($T>T_B$=264 K)	−12.1±0.1	196.1±2.5	4.1±0.3	
4	−13+05±0.03	195.3±0.3	7.9±0.1	81±2
10	−10.9±0.2	238±4	6.1±0.5	75±10
1.500[b]	−11±1.9	337±14	3.8±1.9	115±16

[a]Calculated using $\tau(T_g)=100$ s.
[b]From data of Theobald *et al.* (Ref. 65).

where ε_0 (=8.854 19 pF/m) is the vacuum permittivity and ω the angular frequency. In Fig. 3 this conductivity at atmospheric pressure is shown as a function of temperature. In the insert to Fig. 3 a plot of $\log(\sigma)$ vs $\log(\tau_\alpha)$ shows the expected inverse correlation of two quantities, with a linear coefficient close to −1 over most of the range. However, for the trimer and tetramer, some deviation is evident at $\tau_\alpha \sim 10^{-3}$ s, with a smaller slope indicating that σ is decreasing more slowly than τ_α^{-1} as T is reduced.

The usual interpretation of a relationship between σ and τ_α comes from the consideration of a simple hydrodynamic model for macroscopic (Brownian) particles. The product of the rotational relaxation time and the diffusion constant D_T is constant according to the classical Stokes-Einstein and Debye-Stokes-Einstein equations. These equations have been successfully applied to molecular motions in (low viscosity) liquids and to probes in a host of molecules having similar or smaller size.[52–54] The conductivity is proportional to the diffusion constant of the ions D_i (Nernst-Einstein relation),[55]

$$D_i = \frac{\sigma kT}{ec}, \tag{6}$$

where e and c are the charge and concentration of the ions respectively. For a supercooled liquid D_i and σ change by several orders of magnitude over a small range of T, while the change of c is negligible (but not necessarily zero[56]); thus, $D_i\sigma \sim$ const. Therefore, assuming $D_T \sim D_i$, then $\sigma\tau$ should be about constant.[57]

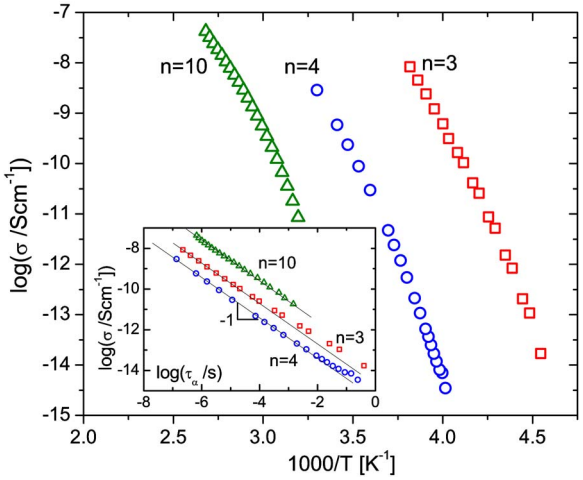

FIG. 3. dc conductivity vs reciprocal temperature for PMMA having the indicated degree of polymerization. In the inset is plotted the conductivity vs segmental relaxation time; the solid line indicates a slope of minus unity.

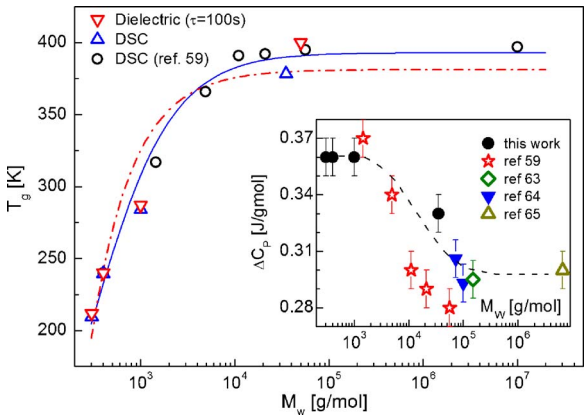

FIG. 4. Molecular weight dependence of atmosphere pressure T_g measured herein by calorimetry and dielectric relaxation [$\tau(T_g)=100$ s], and from DSC measurements of Andreozzi *et al.* (Ref. 61). The solid and dotted lines are the respective best fits to the UK ($T_{g,\infty}$=393±4 K, k_{UK} =0.7±0.04 g mol^{-1} K^{-1}) and FF ($T_{g,\infty}$=381±8 K, k_{FF}=(5.6±0.4) ×10^4 g mol^{-1} K) equations. The inset shows the change with molecular weight of the heat capacity at the glass transition from measurements herein and literature data (Refs. 61 and 65–67). The dotted line is to guide the eyes.

The behavior in the insert of Fig. 3 is mostly consistent with $\sigma\tau \sim$ const, while the deviation observed for the trimer and tetramer suggests a possible decoupling of translational and rotational motions for $\tau_\alpha > 10^{-3}$ s, which is still far from the glass transition. A similar decoupling, manifested as an enhancement in the translational diffusion coefficient relative to the rate of rotational diffusion, has been reported at temperatures below $1.2T_g$ in various supercooled systems,[58,59] although recent numerical simulations suggest the need for a critical reexamination of this issue.[60]

Glass transition temperature

In Fig. 4 is shown the variation of the glass transition temperature with M_w as determined from calorimetry and dielectric measurements, using $\tau(T_g)=100$ s for the latter (for the decamer extrapolation of the fitted VFTH equation was required). Also included in the figure are literature results from DSC measurements of Andreozzi *et al.*[61] There is good consistency among the different measurements, with T_g exhibiting a strong dependence on chain length for $M_w < 10^4$ g/mol. Generally, this dependence of T_g on molecular weight is small for flexible chain polymers such as PDMS,[9] while more rigid or bulky polymers, for example polystyrene, have strongly M_w-dependent glass temperatures.[11] The usual interpretation is that chain ends confer extra unoccupied space ("free volume"), which has a large influence on T_g for a rigid or bulky chain. This role of chain ends on T_g is corroborated by studies of bidisperse polymer blends.[62] From free volume ideas Fox and Flory[63] derived an expression for the variation of the T_g of linear polymers with number average of molecular weight (M_n),

$$T_g = T_{g,\infty} - k_{FF}/M_n, \tag{7}$$

where $T_{g,\infty}$ is the limiting value of the glass transition temperature and k_{FF} is a constant dependent on the chemical structure. A more accurate empirical expression was proposed by Ueberreiter and Kanig[64] (UK),

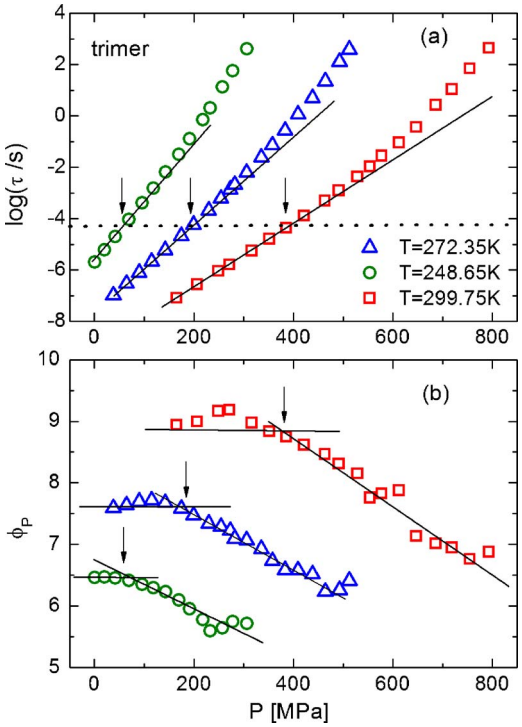

FIG. 5. (a) Isothermal segmental relaxation times vs pressure for the trimer. (b) derivative function for the pressure dependence; solid lines are a guide to the eyes.

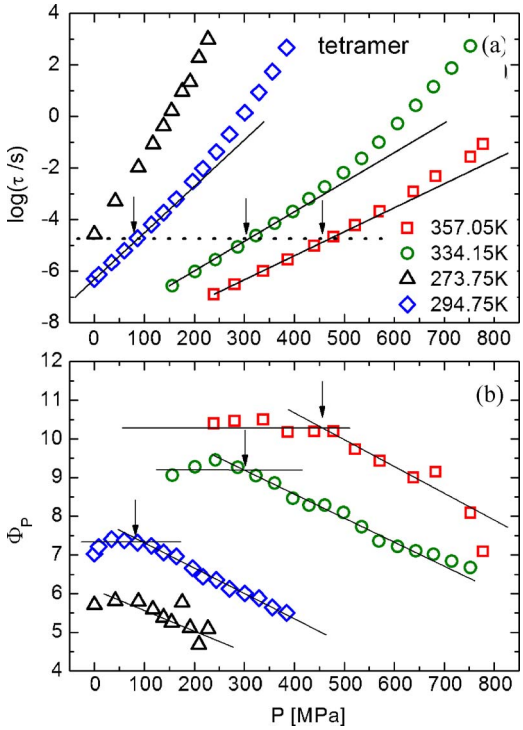

FIG. 6. (a) Isothermal segmental relaxation time vs pressure for the tetramer. (b) derivative function for the pressure dependence; solid lines are a guide to the eyes.

$$T_g^{-1} = T_{g,\infty}^{-1} + k_{\mathrm{UK}}/M_n, \tag{8}$$

in which k_{UK} is a constant.

In Fig. 4 we show the fits of both equations, with the UK equation giving a better description of the data. The inset in Fig. 4 shows the change of the heat capacity at the glass transition, ΔC_P, vs M_w, including some literature data.[61,65–67] For low molecular weights ($<10^3$ g/mol), the heat capacity jump at the glass transition is constant within the limit experimental error, $\Delta C_P = 0.35 \pm 0.01$ J g^{-1} K^{-1}. For higher M_w (>1 kg/mol), ΔC_P decreases with molecular weight, in agreement with previous work, showing ΔC_P for PMMA decreasing from 0.37 to 0.28 J/g C for M_w in the range of 1.45–55.9 kg/mol.[61] Results for other polymers are mixed: For PDMS (Ref. 9) ΔC_P is independent of M_w, while for PS[3] ΔC_P decreases with increasing M_w.

The fragility, characterizing the temperature dependence of τ_α close to T_g, was found to increase with molecular weight from 74 ± 2 for the trimer to substantially higher values for the high polymer, $m = 115 \pm 16$ (Ref. 65) and $m = 145$.[68] A difference in fragility between low and high M_w PMMA was preliminarily reported by Ding *et al.*[6] The trend is similar to that observed for other polymers, as discussed in the Introduction. As suggested by Angell,[1,69] the fragility of liquids reflects the topology of the potential energy hypersurface governing the dynamics. This implies that more fragile liquids are associated with potential surfaces having a high density of minima, and hence a high configurational heat capacity change at T_g. However, the situation is complex, so that a simple correlation between m and $\Delta C_P(T_g)$ is not realized.[70,71] Indeed we have shown for polymers that the two quantities are often anti-correlated for samples differing only in molecular weight.[9,68,72] Thus, the results herein confirm that the change of m with M_w is anti-correlated with the change of ΔC_P with M_w.

Pressure dependence of τ_α

In Figs. 5–7 the logarithm of τ_α measured at various temperatures for the three samples is plotted versus pressure. In all cases the behavior is linear at low pressures, with the pressure sensitivity increasing for larger τ_α. For low pressures

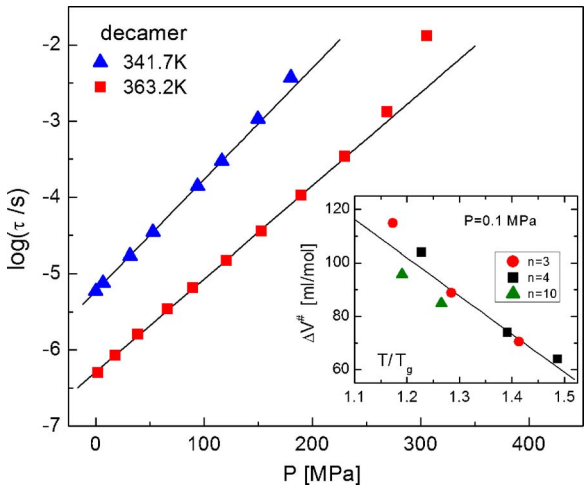

FIG. 7. Isothermal segmental relaxation time vs pressure for the decamer. The insert shows the activation volume in the limit of zero pressure as a function of temperature normalized by the glass temperature (at $P = 0.1$ MPa). ΔV was determined from linear fits of the isothermal $\log(\tau_\alpha)$ vs pressure data for the three oligomers; solid line is a linear fit.

$$\tau_\alpha(P) = \tau_0 \exp(P\Delta V^{\#}/RT), \tag{9}$$

where $\Delta V^{\#}$ is the activation volume and R the gas constant. Alternatively, the activation volume can be expressed as

$$\Delta V^{\#} = -RT\kappa_T \left.\frac{\partial \ln(\tau_\alpha)}{\partial \ln(V)}\right|_T, \tag{10}$$

where $\kappa_T(=-(1/V)(\partial V/\partial P)|_T)$ is the isothermal compressibility. Equation (10) shows directly the relationship between τ_α and V. If the scaling [Eq. (1)] is valid, it then follows that

$$\left.\frac{\partial \ln(\tau_\alpha)}{\partial \ln(V)}\right|_T = \left.\frac{\partial \ln(\tau_\alpha)}{\partial T}\right|_V T\gamma = -\frac{\gamma}{T}\left.\frac{\partial \ln(\tau_\alpha)}{\partial (1/T)}\right|_V = -\gamma m_V(T), \tag{11}$$

where $m_v(T)$ is the T_g-normalized temperature dependence at fixed V, which for $T=T_g$ is the isochoric fragility. Combining Eqs. (10) and (11), the activation volume is related to the scaling exponent as

$$\Delta V^{\#} = RT\kappa_T m_V \gamma. \tag{12}$$

Since for a given material at fixed τ_α [for example, $\tau_\alpha(T_g)$] m_v is a constant,[36] it follows that the T dependence of the activation volume at fixed τ_α is determined by the product $\kappa_T T$, or equivalently that $\partial \log(\tau)/\partial P|_T \propto k_T$.

If $\log(\tau_\alpha)$ varies nonlinearly with pressure, an equation similar to Eq. (4) with T replaced by inverse pressure has been found to accurately describe the pressure dependence.[22,73] Using the analog of Eq. (5) for the high pressure data,[50,74]

$$\phi_P = \{d[\log(\tau_\alpha)]/dP\}^{-1/2}. \tag{13}$$

For volume-activated behavior ϕ_P is a constant but otherwise varies linearly with P. In Figs. 5(b) and 6(b) is shown the function ϕ_P calculated, respectively, for the trimer and tetramer. In both cases a dynamic crossover is observed, reflected in the change in behavior of ϕ_P. For both materials this crossover occurs at a constant value (to within the error) of the relaxation time, $\log \tau_c(\mathrm{s}) \sim -4 \pm 0.5$, independent of pressure. Interestingly, this τ_c is much larger than the relaxation time, τ_B, at the crossover in the temperature dependence of τ_α (Fig. 2). Previously, dielectric measurements on phenolphthalein-dimethylether and polychlorinated biphenyls[50,75,76] and viscosity measurements on *ortho*-terphenyl and salol[74] indicated that the change in slope in ϕ_P occurs at the same τ_α (or viscosity) as the crossover occurring in ϕ_T. This correspondence between the crossover in ϕ_P and ϕ_T is also evident in the scaling properties [Eq. (1)] for various glass-forming liquids.[36,77] In the present case, however, the high pressure measurements are limited to frequencies below 10^6 Hz, so that the existence of a second crossover in ϕ_P at the shorter τ_B cannot be tested. Supporting this supposition are previous cases[36,50] in which the pressure dependence at the crossover changed from VFTH-like at low pressure to approximately activated behavior at high pressure; the PMMA data in Figs. 5(b) and 6(b) show the opposite behavior. By far the most common behavior is for $\log \tau_\alpha(P)$ to be linearly proportional to P at low P.[78–95]

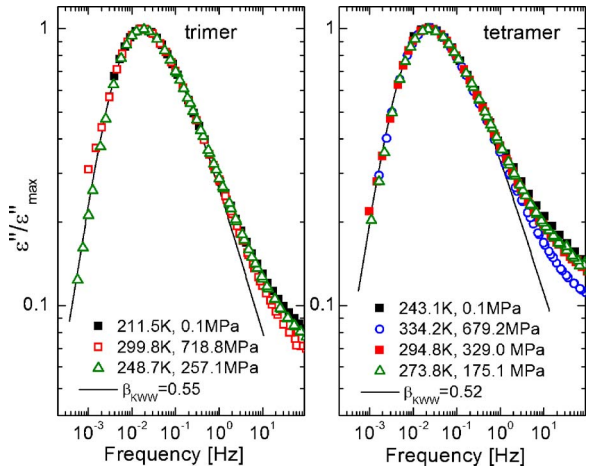

FIG. 8. Comparison of isochronal spectra ($\tau \sim 10$ s) for the trimer and tetramer.

For molecular liquids, in which structural relaxation involves rotation of the molecule, the activation volume, reflecting the unoccupied space necessary for the motion, often has a value close to the molar volume. For polymers, in which structural relaxation corresponds to correlated conformational transitions of several backbone bonds, there is no obvious unit to identify with the local segmental dynamics. Generally, for polymers activation volumes are found to be significantly larger than the volume of the repeat unit.[80,88] Since the PMMA oligomers have the same chemical structure, their respective $\Delta V^{\#}$ should be equivalent. The insert in Fig. 7 shows $\Delta V^{\#}$ in the limit of zero pressure as a function of temperature normalized by the ambient pressure T_g. The values for the three oligomers are quite close.

Local segmental relaxation dispersion

Another important characteristic of structural relaxation is the shape of the dispersion (relaxation function). An equation often used to describe the dispersion is the one-sided Fourier transform of the Kohlrausch function[96,97]

$$\phi_{\mathrm{KWW}}(t) = \exp[-(t/\tau_\alpha)^{\beta_{\mathrm{KWW}}}], \tag{14}$$

where β_{KWW} is the stretching parameter $(0 < \beta_{\mathrm{KWW}} \leqslant 1)$. There is a general correlation between β_{KWW} and m for atmospheric pressure,[2] with larger values of fragility associated with broader dispersions. Although within a given class of glass formers the correlation is at least approximately valid, exceptions abound more generally.[98] For nonassociated materials at elevated pressure, m usually decreases,[36] while β_{KWW} is unchanged for conditions of T and P such that τ_α is constant.[99,100]

In Fig. 8 we show spectra for the trimer and tetramer measured at different T and P chosen such that the $\tau_\alpha \sim 10$ s. Good superpositioning of the peaks is found, in accord with the behavior of other glass formers, both molecular and polymeric.[99,100] The fit of Eq. (14) (shown as solid lines in Fig. 8) yields $\beta_{\mathrm{KWW}}=0.52$ for the tetramer and $\beta_{\mathrm{KWW}}=0.55$ for the trimer. Thus, the more fragile material has a smaller β_{KWW}, in accord with the general pattern.[2] For the decamer the intensity of the secondary relaxation is rela-

TABLE II. Fit parameters for Eq. (15).

n	a_0 (ml/g)	a_1 (ml/g C)	a_2 (ml/g C^2)	b_1 (MPa)	b_2 (C^{-1})
3	0.817±0.0002	$(6.43\pm0.07)\times10^{-4}$	$(5.0\pm0.6)\times10^{-7}$	185±0.6	$(5.2\pm0.05)\times10^{-3}$
4	0.819±0.0002	$(6.33\pm0.06)\times10^{-4}$	$(5.2\pm0.6)\times10^{-7}$	191±0.6	$(4.7\pm0.05)\times10^{-3}$
10	0.818±0.0001	$(6.05\pm0.01)\times10^{-4}$	⋯	235±0.4	$(4.3\pm0.02)\times10^{-3}$
1.500[a]	0.819±0.002	$(3.2\pm0.3)\times10^{-4}$	$(6.1\pm1)\times10^{-7}$	316±8	$(4.6\pm0.1)\times10^{-3}$

[a]From analysis of *PVT* data in Ref. 65.

tively large, so that a distinct loss peak is never isolated away from the secondary relaxation. Since the T and P dependences of the relaxation times and intensities for the two peaks may differ, their deconvolution is necessary to accurately determine the shape of the local segmental peak. However, the proper method to deconvolute is controversial.[43,101–103]

Equation of state

Above the glass transition experimental specific volumes can be represented using the Tait equation of state (EOS),

$$V(T,P) = (a_0 + a_1 T + a_2 T^2) \times \left\{ 1 - 0.894 \ln\left[1 + \frac{P}{b_1 \exp(-b_2 T)} \right] \right\}, \quad (15)$$

where a_0, a_1, a_2, b_1, and b_2 are constants having the values listed in Table II. (By convention temperature is in units of °C.) Using the respective EOS, τ_α for each sample is obtained as a function of V (Fig. 9). As found for virtually all glass-forming materials,[22] the relaxation times are not defined solely by V. However, the data do superimpose when plotted versus the TV^γ (Fig. 10). Also included in Fig. 10 are τ_α for a high molecular weight PMMA (M_w=1.5 $\times10^5$ g/mol) measured by Theobald *et al.*[65] We find that the scaling exponent decreases with increasing molecular weight: γ=3.7, 3.2, 2.8, and 1.8 for the trimer, tetramer, decamer, and high polymer, respectively. In the case of high M_w, PMMA it is possible to determine the pressure dependence of T_g from *PVT* measurements and estimate γ. The ratio E_V/H_P can be calculated using[80]

$$\frac{E_V}{H_P} = \frac{1}{1 - \alpha_P/\alpha_\tau}, \quad (16)$$

where $\alpha_\tau (= \partial \ln(V)/\partial T|_\tau)$ is the isochronic thermal expansion coefficient. For high M_w PMMA we find α_τ=(−1.4±0.2) $\times10^{-3}$ C^{-1}, from which we calculated E_V/H_P=0.73±0.03. From Eq. (3) we then calculate $\gamma=-(\alpha_r T_g)^{-1}$=1.85±0.25, which is in good agreement with γ found by superpositioning the τ data. In the literature we found that a somewhat lower value of γ=1.25 was reported for a different high M_w PMMA (Ref. 104), but no details were provided concerning the molecular weight or tacticity of the sample used in that study.

For the trimer γ is close to the value for van der Waals molecular glass formers such as orthoterphenyl (γ=4),[105] propylene carbonate (γ=3.7),[106] cresolphthalein-dimethylether (γ=4.5),[77] phenylphthalein-dimethylether (γ=4.5),[24] and decahydroisoquinoline (γ=3.55),[107] although values of γ as high as 8.5 have been found for bulkier molecular liquids, such as 1,1′-di(4-methoxy-5-methylphenyl)cyclohexane[24] and polychlorinated biphenyls.[94]

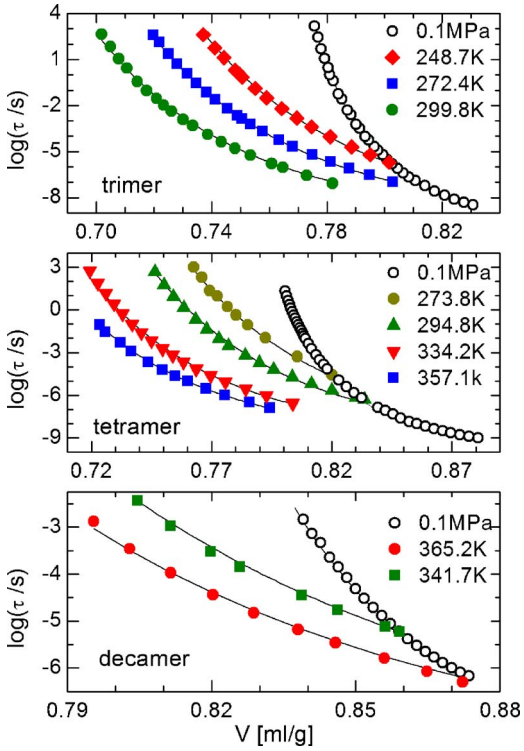

FIG. 9. Isothermal and isobaric segmental relaxation times vs volume for the three oligomers. The solid lines represent the fit to Eq. (24).

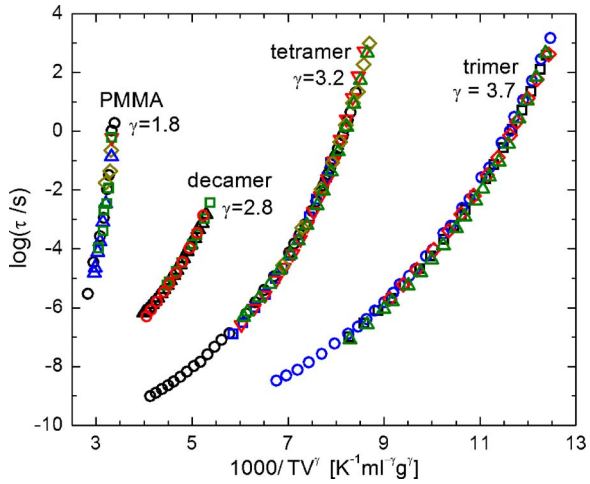

FIG. 10. Scaling plots of the segmental relaxation times for the three oligomers and a high molecular weight PMMA [the latter from Theobald *et al.* (Ref. 65)]. Each symbol type corresponds to a curve in Fig. 9.

TABLE III. Thermodynamic parameters: glass transition temperature, T_g; isobaric expansion coefficient, α_P; isothermal compressibility, κ_T; specific volume at T_g, V_g; activation volume at T_g, $\Delta V_g^{\#}$; scaling exponent for the relaxation times, γ, ratio of the isochoric and isobaric activation enthalpies [Eq. (3)]; change of the isobaric heat capacity at the glass transition; and scaling exponent for S_c calculated as $\gamma_{S_c}=V\alpha_P/\kappa_T\Delta C_P$.

n	T_g (K)	$\alpha_P\times10^{-4}$ (K^{-1})	$\alpha_T\times10^{-4}$ (MPa^{-1})	V_g (ml g^{-1})	ΔV_g (ml mol^{-1})	$\Delta V_g^{\#}/kT_g$ (kJ mol^{-1} K^{-1})	γ	$E_V/H_P\vert_{Tg}$	$\Delta C_P\vert_{Tg}$ (J K^{-1} g^{-1})	γ_{S_c}
3	209.6	7.48	3.47	0.774	132±9	1.8±0.1	3.7	0.63	0.36	4.6
4	239.6	7.50	4.00	0.797	130±3	1.4±0.1	3.2	0.63	0.36	4.1
10	287.9	7.32	4.05	0.827	128±17	1.1±0.1	2.8	0.63	0.36	4.1
1500	379.8	5.24	4.62	0.860	216±30	1.2±0.2	1.8	0.74	0.29	3.3

DISCUSSION

This study of PMMA illustrates that chain length exerts a strong influence on local segmental relaxation properties, in particular the relative effect of T and V on the dynamics. In going from the trimer to the high polymer, the effect of volume is suppressed, as reflected in the decrease of γ from 3.7 to 1.8. (Although the contribution of V relative to T, as measured by the T- and V-dependent metric E_V/H_P in Table II, shows negligible change among the three oligomers when evaluated at T_g.) Qualitatively, we ascribe this variation of the scaling exponent with molecular weight to a softening of the repulsive potential due to an increasing influence of the intrachain potential. There is a concomitant reduction in the packing efficiency with M_w, as seen in the increasing volume at the glass transition, V_g, with M_w (Table III). These chain length dependences are consistent with the relative stiffness of the PMMA chain.

In Table III are listed the activation volumes for the three oligomers and the high molecular weight PMMA, as obtained using Eq. (12). The larger $\Delta V^{\#}$ for the high polymer follows from its higher T_g and larger κ_T. The molar volume of the repeat unit in PMMA determined at T_g using the EOS [Eq. (15)] are 78, 80, and 83 ml/mol for $n=3$, 4, and 10, respectively, which is about 50% smaller than $\Delta V^{\#}$. Another obvious difference in comparing $\Delta V^{\#}$ with the actual volume is that while V increases with increasing T, $\Delta V^{\#}$ decreases; thus, in the limit of high $T(\sim1.3T_g)$ the two have comparable magnitudes. This is consistent with results for other polymers.[20,108,109]

Previously, we showed for propylene carbonate, salol, polyvinylacetate, *o*-terphenyl, and a mixture of *o*-terphenyl with *o*-phenyl phenol that the entropy is well represented by[27,28]

$$S=f(TV^{\gamma_S}), \tag{17}$$

with the scaling exponent γ_S bearing a relationship to the Grüneisen parameter, γ_G, defined as

$$\gamma_G=\frac{V\alpha_P}{C_V\kappa_T}. \tag{18}$$

Thus, the condition $TV^{\gamma_S}=$const corresponds to a reversible adiabatic transformation reminiscent of an ideal gas. Interestingly, the scaling exponent for the relaxation times, γ, is about threefold larger than γ_G,[26–28] due to nonconfigurational contributions to the entropy from vibrational and local secondary motions, which do not affect structural relaxation.

It is reasonable to assume that in the liquid state during an isothermal volume change, the entropy change is purely configurational; that is, the unoccupied or free volume has to be removed before vibrational or local intramolecular motions are affected. A simple parallel is that of a soft matrix containing hard particles—compressing the matrix is not expected to appreciably change the particle volume *per se*. In this approximation then,

$$\left.\frac{\partial S_c}{\partial V}\right|_T=\left.\frac{\partial S_{\mathrm{liq}}}{\partial V}\right|_T-\left.\frac{\partial S_0}{\partial V}\right|_T\approx\left.\frac{\partial S_{\mathrm{liq}}}{\partial V}\right|_T, \tag{19}$$

where S_{liq} is the total entropy of the liquid, S_c the entropy in excess of that from vibrational or local intramolecular motions, and S_0 the nonconfigurational entropy. S_c is calculated starting from the differential form

$$\begin{aligned}dS_c&=\left(\left.\frac{\partial S_{\mathrm{liq}}}{\partial T}\right|_V-\left.\frac{\partial S_0}{\partial T}\right|_V\right)dT+\left(\left.\frac{\partial S_{\mathrm{liq}}}{\partial V}\right|_T\right)dV\\&=\frac{\Delta C_V}{T}dT+\left.\frac{\partial P_{\mathrm{liq}}}{\partial T}\right|_V dV,\end{aligned} \tag{20}$$

where we have used Eq. (19) together with one of the Maxwell relations, and $\Delta C_V=C_V^{\mathrm{liq}}-C_V^{\mathrm{non}}$. Defining the Grüneisen parameter for S_c, γ_{S_c}, as

$$\gamma_{S_c}=\frac{V\alpha_P^{\mathrm{liq}}}{\Delta C_V\kappa_T^{\mathrm{liq}}}, \tag{21}$$

Eq. (20) can be rewritten as

$$dS_c=\Delta C_V\left(\frac{dT}{T}+\gamma_{S_c}\frac{dV}{V}\right). \tag{22}$$

If γ_{S_c} and ΔC_V are independent of V and T, respectively, the integration of Eq. (22) gives

$$S_c=\Delta C_V\ln(TV^{\gamma_{S_c}})+\mathrm{const}. \tag{23}$$

This shows that S_c scales as a function of the variable $TV^{\gamma_{S_c}}$, in the manner that τ_α, does, which implies an entropy basis for the glass transition dynamics.

In Table III are the values of γ_{S_c} calculated using Eq. (21). Since the PMMA are atactic, there is no crystallinity and so the available reference state is the glass. This approximation underestimates S_c since some configurational degrees of freedom may not be frozen in the glass (possibly being manifested as secondary relaxations). Since $V(T,P)$ data are unavailable for the samples below T_g, we make the further approximation that $C_V^{\mathrm{glass}}\sim C_P^{\mathrm{glass}}$; thus, we take $\Delta C_V\cong C_P^{\mathrm{liq}}-C_P^{\mathrm{glass}}$. The obtained γ_{S_c} are larger than the values of γ that

TABLE IV. Fit parameters for Eq. (24) (shown as solid lines in Fig. 9).

n	A	B	D	γ_A
3	−9.53±0.08	83.3±0.2	3.91±0.06	3.60±0.01
4	−9.30±0.07	116.2±0.4	4.07±0.06	3.22±0.01
10	−8.5±0.2	163.4±1.2	3.1±0.2	2.98±0.04

scale τ_α; however, both decrease in a similar fashion with increasing M_w, unlike ΔC_P, which is approximately constant for different materials. This variation with M_w could be related to the increasing contribution of the secondary relaxation to the entropy, which causes ΔC_V and S_c to be underestimated.[110] Note that the difference between γ_{S_c} and γ increases with M_w, in parallel with the increase of the relative strength of the secondary relaxation.[111]

The best known model for the glass transition is due to Adam and Gibbs,[112,113] which predicts τ_α to be a function of the product TS_c. In typical measurements near the glass transition, τ_α changes by approximately eight orders of magnitude, while T changes by around 20% and S_c by about two orders of magnitude. The implication is that the dynamics are dominated by changes of S_c. A variation on the model of Adam and Gibbs is due to Avramov.[114] Starting from the Avramov model, we have shown that using Eq. (23) for the entropy, the following expression for $\tau_\alpha(T,V)$ is obtained[26]

$$\log[\tau(T,V)] = A + \left(\frac{B}{TV^{\gamma_A}}\right)^D, \tag{24}$$

where A, B, D, and γ_A are constants. This equation, shown in Fig. 9 as solid lines, accurately describes the τ_α over a broad dynamic range, with the obtained parameters given in Table IV. The γ_A determined from fitting Eq. (24) are essentially equivalent to the γ obtained by superpositioning the τ_α data.

In assessing entropy models for polymers, there is a lack of connection between the magnitude of the heat capacity change at T_g and the variation of fragility with M_w.[68,72] However, considering both the T and V dependences of $S_c(T,V)$, the calculated value of γ_{S_c} is close to that of γ and has the same trend with changing M_w. In fact γ_{S_c} depends inversely on ΔC_P and directly on the ratio α_P/κ_T, and in the same manner as γ, decreases with increasing M_w. The change of ΔC_P from low to high M_w is only ~10%, while the change of the ratio α_P/κ_T is about one-half, similar to the change in γ.

Application of Eq. (5) indicates a crossover for the trimer and, more weakly, for the tetramer, at a relaxation time $\tau_B \sim 10^{-7}$ s (Fig. 2). This crossover time was found to be independent of pressure in other materials,[50,74] but this P independence could not be investigated herein because of the limited frequency range of the high pressure measurements. However, using Eq. (13), a second crossover is found at a much lower frequency, on the order of $\tau_c \sim 10^{-4}$ s (Figs. 5 and 6). This pressure crossover transpires between the volume-activated dynamics at short times ($\Delta V^\# \sim$ const) and the VFTH-like dependence at longer times ($\Delta V^\#$ increases with P). This is different from the pressure crossover behavior found previously, for which there was a correspondence between the relaxation times from Eqs. (5) and (13). Since

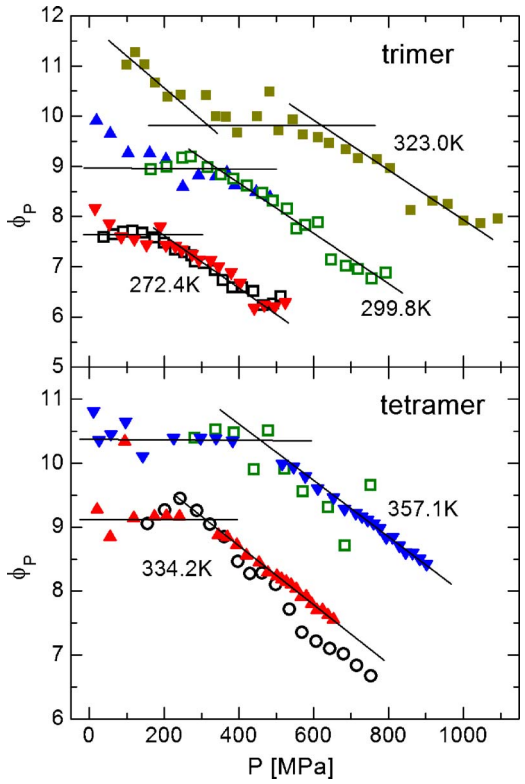

FIG. 11. Derivative function for the pressure dependence of the trimer and tetramer. The open symbols were calculated from the isothermal measurements (as in Figs. 5 and 6), while the solid symbols were calculated from the atmospheric data using the scaling properties (see text). Solid lines are to guide the eyes.

the TV^γ scaling [Eq. (1)] applies to the trimer and tetramer, we can use the atmospheric pressure data for $\tau_\alpha(T,V)|_{P=0.1\ \mathrm{MPa}}$ (which could be determined over a broad range) together with the EOS to calculate the isothermal behavior, $\tau_\alpha(P,V)|_{T=\mathrm{const}}$. [This procedure interpolates the relaxation time data using Eq. (1) as the interpolation function.[36]] For a given temperature $T=T_A$, this is done first using Eq. (1) to calculate for each $\tau_\alpha(T,V)|_{P=0.1\ \mathrm{MPa}}$ the corresponding value of V at $T=T_A$ having the same value of the relaxation time, $\tau_\alpha(P,V)|_{T=T_A}$. Then the corresponding pressure $P(T_A,V)$ is obtained from the EOS (negative pressure results were not considered). As shown previously for other materials,[36] this procedure yields an accurate set of isothermal τ_α, from which the crossover could be determined. Equation (13) is applied to these data, as shown in Fig. 11 as solid symbols, together with the ϕ_P in Figs. 5 and 6 calculated from the actual high pressure measurements (open symbols). The consistency between these two sets of data (in their common range of P) shows that the behavior is intrinsic to the atmospheric pressure and EOS results. Note that for the trimer there is a hint of a second crossover at $\tau \sim \tau_B$, at least for the higher T data set. The second crossover at longer τ_α could be a signature of the splitting of the local segmental and secondary relaxations. This will be the subject of future work.[111]

CONCLUSIONS

The structural dynamics of PMMA oligomers (n=3, 4, and 10) was studied over a wide range of frequency as a

function of T, P, and V. The dependence of the structural relaxation on T and V is strongly influenced by the chain length, as reflected in the variation of γ with M_w. For the smallest polymer chain (trimer), the scaling exponent is very close to that for van der Walls liquids ($\gamma \sim 4$), and it decreases with increasing M_w to $\gamma = 1.8$ for the high polymer. This shows that small values of the scaling parameter, as generally observed for polymers,[22] are mainly due to the relative stiffness of the backbone units, in comparison to the mobility arising from intermolecular degrees of freedom. We also find, consistent with previous works for a given family of materials,[115–117] a similar effect of M_w on other dynamic properties, such as the fragility and the glass transition temperature, and on thermodynamic parameters, such as the heat capacity change and the specific volume at T_g. The chain structure hinders segmental rearrangements with a consequent smaller sensitivity to intermolecular distance and larger V. Conversely, polymers having a very flexible chain (e.g., siloxane polymers) are associated with larger values of $\gamma(\sim 5)$ and near invariance of m and T_g to M_w.

Using the derivation function [Eq. (5)], we observed a crossover in the temperature dependence of the relaxation times at atmospheric pressure for the trimer and tetramer at $\tau_B \sim 10^{-7}$ s. However, for the latter, this crossover is weaker, suggesting that for sufficiently high M_w it may eventually "disappear." Unfortunately for high M_w PMMA, the substantial intensity of the secondary relaxation precludes testing this supposition. Using Eq. (13), we observe both the crossover around $\tau_\alpha \sim \tau_B$ and a second crossover at much longer τ_α ($\sim 10^{-4}$ s). The latter does not seem to have a counterpart in the T behavior of ϕ_T. However, at this same value of the relaxation time there is a decoupling between the conductivity and the local segmental relaxation (inset in Fig. 3).

Finally, for the PMMA oligomers we find that the shape of the relaxation dispersion, as described using a KWW function, is constant for a given value of the relaxation time; that is, the segmental dispersion is invariant to different thermodynamical conditions at constant τ_α. Together with the scaling [Eq. (1)], this means that γ determines both the relaxation time and the breadth of its distribution.

ACKNOWLEDGMENTS

This work was supported by the Office of Naval Research and by MIUR (PRIN 2005). The authors thank K. J. McGrath for providing *PVT* data and L. J. Buckley for use of the HP4291A impedance analyzer.

[1] C. A. Angell, in *Relaxation in Complex Systems*, edited by K. L. Ngai and G. B. Wright (Government Printing Office, Washington, DC, 1985).
[2] R. Böhmer, K. L. Ngai, C. A. Angell, and D. J. Plazek, J. Chem. Phys. **99**, 4201 (1993).
[3] P. G. Santangelo and C. M. Roland, Macromolecules **31**, 4581 (1998).
[4] C. G. Robertson, P. G. Santangelo, and C. M. Roland, J. Non-Cryst. Solids **275**, 163 (2000).
[5] C. M. Roland and R. Casalini, J. Chem. Phys. **119**, 1838 (2003).
[6] Y. Ding, V. N. Novikov, A. P. Sokolov, A. Calliaux, C. Dalle-Ferrier, C. Alba-Simionesco, and B. Frick, Macromolecules **37**, 9264 (2004).
[7] C. Leon, K. L. Ngai, and C. M. Roland, J. Chem. Phys. **110**, 11585 (1999).
[8] J. Mattsson, R. Bergman, P. Jacobsson, and L. Börjesson, Phys. Rev. Lett. **90**, 075702 (2003).
[9] C. M. Roland and K. L. Ngai, Macromolecules **29**, 5747 (1996).
[10] S. Pawlus, S. J. Rzoska, J. Ziolo, M. Paluch, and C. M. Roland, Rubber Chem. Technol. **76**, 1106 (2003).
[11] K. L. Ngai and C. M. Roland, Macromolecules **26**, 6824 (1993).
[12] C. M. Roland, Macromolecules **27**, 4242 (1994).
[13] C. M. Roland, K. J. McGrath, and R. Casalini, J. Non-Cryst. Solids **352**, 4910 (2006).
[14] G. Williams, in *Dielectric Spectroscopy of Polymeric Materials*, edited by J. P. Runt and J. J. Fitzgerald (American Chemical Society, Washington, DC, 1997).
[15] P. Papadopoulos, D. Peristeraki, G. Floudas, G. Koutalas, and N. Hadjichristidis, Macromolecules **37**, 8116 (2005).
[16] C. Dreyfus, A. Aouadi, J. Gapinski, W. Steffen, M. Matos-Lopes, A. Patkowski, and R. M. Pick, Eur. Phys. J. B **42**, 309 (2004).
[17] M. Paluch, R. Casalini, A. Best, and A. Patkowski, J. Chem. Phys. **117**, 7624 (2002).
[18] K. Mpoukouvalas and G. Floudas, Phys. Rev. E **68**, 031801 (2003).
[19] C. M. Roland, M. Paluch, T. Pakula, and R. Casalini, Philos. Mag. **84**, 1573 (2004).
[20] M. Paluch, R. Casalini, A. Patkowski, T. Pakula, and C. M. Roland, Phys. Rev. E **68**, 031802 (2003).
[21] M. Paluch, C. M. Roland, R. Casalini, G. Meier, and A. Patkowski, J. Chem. Phys. **118**, 4578 (2003).
[22] C. M. Roland, S. Hensel-Bielowka, M. Paluch, and R. Casalini, Rep. Prog. Phys. **68**, 1405 (2005).
[23] C. M. Roland and R. Casalini, Macromolecules **38**, 8729 (2005).
[24] R. Casalini and C. M. Roland, Phys. Rev. E **69**, 062501 (2004).
[25] C. M. Roland, S. Bair, and R. Casalini, J. Chem. Phys. **125**, 124508 (2006).
[26] R. Casalini, U. Mohanty, and C. M. Roland, J. Chem. Phys. **125**, 014505 (2006).
[27] R. Casalini and C. M. Roland, Philos. Mag. **87**, 459 (2007).
[28] C. M. Roland and R. Casalini, J. Phys.: Condens. Matter (in press) (e-print cond-mat/0610428).
[29] J. D. Weeks, D. Chandler, and H. C. Andersen, J. Chem. Phys. **54**, 5237 (1971).
[30] M. S. Shell, P. G. Debenedetti, E. La Nave, and F. Sciortino, J. Chem. Phys. **118**, 8821 (2003).
[31] N. H. March and M. P. Tosi, *Introduction to Liquid State Physics* (World Scientific, Singapore, 2002).
[32] W. G. Hoover and M. Ross, Contemp. Phys. **12**, 339 (1971).
[33] P. G. Debenedetti, F. H. Stillinger, T. M. Truskett, and C. J. Roberts, J. Phys. Chem. B **103**, 7390 (1999).
[34] G. Tsolou, V. G. Mavrantzas, and D. N. Theodorou, Macromolecules **38**, 1478 (2005).
[35] G. Tsolou, V. A. Harmandaris, and V. G. Mavrantzas, J. Chem. Phys. **124**, 084906 (2006).
[36] R. Casalini and C. M. Roland, Phys. Rev. B **71**, 014210 (2005).
[37] D. W. Van Krevelen, *Properties of Polymers* (Elsevier, New York, 1990).
[38] R. F. Boyer and R. S. Spencer, J. Appl. Phys. **15**, 398 (1944).
[39] C. M. Roland, D. F. Roland, J. Wang, and R. Casalini, J. Chem. Phys. **123**, 204905 (2005).
[40] P. Zoller and D. J. Walsh, *Standard Pressure-Volume-Temperature Data for Polymers* (Technomic, Lancaster, PA, 1995).
[41] D. A. Ditmars, S. Ishihara, S. S. Chang, G. Bernstein, and E. D. West, J. Res. Natl. Bur. Stand. **87**, 159 (1982).
[42] H. Sasabe and S. Saito, J. Polym. Sci., Part A-2 **6**, 1401 (1968).
[43] R. Bergman, F. Alvarez, A. Alegria, and J. Colmenero, J. Chem. Phys. **109**, 7546 (1998).
[44] A. Schonhals, in *Broadband Dielectric Spectroscopy*, edited by F. Kremer and A. Schonhals (Springer-Verlag, Berlin, 2003).
[45] H. Vogel, Phys. Z. **22**, 645 (1921).
[46] G. S. Fulcher, J. Am. Ceram. Soc. **8**, 339 (1923).
[47] D. J. Plazek and J. H. Magill, J. Chem. Phys. **45**, 3038 (1966).
[48] A. J. Barlow, J. Lamb, and A. J. Matheson, Proc. R. Soc. London, Ser. A **292**, 322 (1966).
[49] F. Stickel, E. W. Fischer, and R. Richert, J. Chem. Phys. **102**, 6251 (1995).
[50] R. Casalini, M. Paluch, and C. M. Roland, J. Chem. Phys. **118**, 5701 (2003).
[51] V. N. Novikov and A. P. Sokolov, Phys. Rev. E **67**, 031507 (2003).
[52] M. T. Cicerone and M. D. Ediger, J. Phys. Chem. **97**, 10489 (1993).
[53] M. T. Cicerone, F. R. Blackburn, and M. D. Ediger, J. Chem. Phys. **102**, 471 (1995).

[54] J. R. Rajian, W. Huang, R. Richert, and E. L. Quitevis, J. Chem. Phys. **124**, 014510 (2006).
[55] H. J. V. Tyrell and K. R. Harris, *Diffusion in Liquids* (Butterworths, London, 1984).
[56] G. Johari and O. Andersson, J. Chem. Phys. **125**, 124501 (2006).
[57] F. Stickel, E. W. Fischer, and R. Richert, J. Chem. Phys. **104**, 2043 (1995).
[58] F. Fujara, B. Geil, H. Sillescu, and G. Fleischer, Z. Phys. B: Condens. Matter **88**, 195 (1992).
[59] M. K. Mapes, S. F. Swallen, and M. D. Ediger, J. Phys. Chem. B **110**, 507 (2006).
[60] T. G. Lombardo and P. G. Debenedetti, J. Chem. Phys. **125**, 174507 (2006).
[61] L. Andreozzi, M. Faetti, M. Giordano, and F. Zulli, Macromolecules **38**, 6056 (2005).
[62] C. G. Robertson and C. M. Roland, J. Polym. Sci., Part B: Polym. Phys. **42**, 2604 (2004).
[63] T. G. Fox and P. J. Flory, J. Polym. Sci. **14**, 315 (1954).
[64] K. Ueberreiter and G. Kanig, J. Colloid Sci. **7**, 569 (1952).
[65] S. Theobald, W. Pechhold, and B. Stoll, Polymer **42**, 289 (2001).
[66] J. J. Tribone, J. M. O'Reilly, and J. Greener, Macromolecules **19**, 1732 (1986).
[67] E. Hempel, M. Beiner, T. Renner, and E. Donth, Acta Polym. **47**, 525 (1997).
[68] C. M. Roland, P. G. Santangelo, and K. L. Ngai, J. Chem. Phys. **111**, 5593 (1999).
[69] C. A. Angell, Science **267**, 1924 (1995).
[70] C. A. Angell, P. H. Poole, and J. Shao, Nuovo Cimento Soc. Ital. Fis., D **16D**, 883 (1994).
[71] L. M. Wang, C. A. Angell, and R. Richert, J. Chem. Phys. **125**, 074505 (2006).
[72] P. G. Santangelo and C. M. Roland, Phys. Rev. B **58**, 14121 (1998).
[73] G. P. Johari and E. Whalley, Faraday Symp. Chem. Soc. **6**, 23 (1972).
[74] R. Casalini and C. M. Roland, Phys. Rev. Lett. **92**, 245702 (2004).
[75] R. Casalini, M. Paluch, J. J. Fontanella, and C. M. Roland, J. Chem. Phys. **117**, 4901 (2002).
[76] R. Casalini, M. Paluch, and C. M. Roland, J. Phys.: Condens. Matter **15**, s859 (2003).
[77] C. M. Roland and R. Casalini, J. Non-Cryst. Solids **251**, 2581 (2005).
[78] S. Hensel-Bielowka, J. Ziolo, M. Paluch, and C. M. Roland, J. Chem. Phys. **117**, 2317 (2002).
[79] M. Paluch, R. Casalini, S. Hensel-Bielowka, and C. M. Roland, J. Chem. Phys. **116**, 9839 (2002).
[80] R. Casalini and C. M. Roland, J. Chem. Phys. **119**, 4052 (2003).
[81] R. Casalini and C. M. Roland, J. Chem. Phys. **119**, 11951 (2003).
[82] M. Paluch, C. M. Roland, J. Gapinski, and A. Patkowski, J. Chem. Phys. **118**, 3177 (2003).
[83] R. Casalini and C. M. Roland, Phys. Rev. Lett. **91**, 015702 (2003).
[84] S. H. Zhang, R. Casalini, J. Runt, and C. M. Roland, Macromolecules **36**, 9917 (2003).
[85] R. Casalini, M. Paluch, and C. M. Roland, J. Phys. Chem. A **107**, 2369 (2003).
[86] C. M. Roland, T. Psurek, S. Pawlus, and M. Paluch, J. Polym. Sci., Part B: Polym. Phys. **41**, 3047 (2003).
[87] C. M. Roland and R. Casalini, Macromolecules **36**, 1361 (2003).
[88] C. M. Roland, R. Casalini, P. Santangelo, M. Sekula, J. Ziolo, and M. Paluch, Macromolecules **36**, 4954 (2003).
[89] R. Casalini, M. Paluch, and C. M. Roland, Phys. Rev. E **67**, 031505 (2003).
[90] M. Sekula, S. Pawlus, S. Hensel-Bielowka, J. Ziolo, M. Paluch, and C. M. Roland, J. Phys. Chem. B **108**, 4997 (2004).
[91] R. Casalini and C. M. Roland, Phys. Rev. B **69**, 094202 (2004).
[92] C. M. Roland, S. Capaccioli, M. Lucchesi, and R. Casalini, J. Chem. Phys. **120**, 10640 (2004).
[93] S. Maslanka, M. Paluch, W. W. Sulkowski, and C. M. Roland, J. Chem. Phys. **122**, 084511 (2005).
[94] C. M. Roland and R. Casalini, J. Chem. Phys. **122**, 134505 (2005).
[95] C. M. Roland, K. J. McGrath, and R. Casalini, Macromolecules **38**, 1779 (2005).
[96] R. Kohlrausch, Ann. Phys. (Leipzig) **12**, 393 (1847).
[97] G. Williams and D. C. Watts, Trans. Faraday Soc. **66**, 80 (1970).
[98] C. M. Roland, M. Paluch, and S. J. Rzoska, J. Chem. Phys. **119**, 12439 (2003).
[99] K. L. Ngai, R. Casalini, S. Capaccioli, M. Paluch, and C. M. Roland, J. Phys. Chem. B **109**, 17356 (2005).
[100] K. L. Ngai, R. Casalini, S. Capaccioli, M. Paluch, and C. M. Roland, in Adv. Chem. Phys. edited by Y. P. Kalmykov, W. T. Coffey and S. A. Rice (Wiley, New York, 2006), Vol. 133B, Chap. 10.
[101] F. Garwe, A. Schonhals, H. Lockwenz, M. Beiner, K. Schroter, and E. Donth, Macromolecules **29**, 247 (1996).
[102] A. Arbe, D. Richter, J. Colmenero, and B. Farago, Phys. Rev. E **54**, 3853 (1996).
[103] J. C. Dyre and N. B. Olsen, Phys. Rev. Lett. **91**, 155703 (2003).
[104] C. Alba-Simionesco, A. Calliaux, A. Alegria, and G. Tarjus, Europhys. Lett. **68**, 58 (2004).
[105] C. Dreyfus, A. Aouadi, J. Gapinski, M. Matos-Lopes, W. Steffen, A. Patkowski, and R. M. Pick, Phys. Rev. E **68**, 011204 (2003).
[106] S. Pawlus, R. Casalini, C. M. Roland, M. Paluch, S. J. Rzoska, and J. Ziolo, Phys. Rev. E **70**, 061501 (2004).
[107] R. Casalini, K. J. McGrath, and C. M. Roland, J. Non-Cryst. Solids **352**, 4905 (2006).
[108] M. Paluch, S. Pawlus, and C. M. Roland, Macromolecules **35**, 7338 (2002).
[109] H. Kriegs, J. Gapinski, G. Meier, M. Paluch, S. Pawlus, and A. Patkowski, J. Chem. Phys. **124**, 104901 (2006).
[110] D. Cangialosi, A. Alegria, and J. Colmenero, Europhys. Lett. **70**, 614 (2005).
[111] S. Capaccioli, C. M. Roland, and R. Casalini (unpublished).
[112] G. Adam and J. H. Gibbs, J. Chem. Phys. **43**, 139 (1965).
[113] R. Casalini, S. Capaccioli, M. Lucchesi, P. A. Rolla, and S. Corezzi, Phys. Rev. E **63**, 031207 (2001).
[114] I. Avramov, J. Non-Cryst. Solids **262**, 258 (2000).
[115] R. Casalini and C. M. Roland, Phys. Rev. E **72**, 031503 (2005).
[116] R. Casalini, S. Capaccioli, and C. M. Roland, J. Phys. Chem. B **110**, 11491 (2006).
[117] R. Casalini and C. M. Roland, J. Non-Cryst. Solids (in press) (e-print cond-mat/0703518).